The Role of Thr268 in Oxygen Activation of Cytochrome $P450_{BM-3}$[†]

Hyeyeong Yeom and Stephen G. Sligar*

Beckman Institute for Advanced Science and Technology and Department of Biochemistry, University of Illinois, Urbana, Illinois 61801

Huiying Li and Thomas L. Poulos*

Department of Molecular Biology and Biochemistry and Department of Physiology and Biophysics, University of California, Irvine, Irvine, California 92717

Armand J. Fulco

Department of Biological Chemistry, University of California, Los Angeles, School of Medicine, Los Angeles, California 90024

Received June 9, 1995; Revised Manuscript Received August 14, 1995[⊗]

ABSTRACT: Cytochrome $P450_{BM-3}$, a catalytically self-sufficient monooxygenase from *Bacillus megaterium*, catalyzes the ω-n (n = 1−3) hydroxylation of fatty acids in the presence of O_2 and NADPH. Like most other P450s, cytochrome $P450_{BM-3}$ contains a threonine residue (Thr268) in the distal I helix thought to be important for O_2 binding and activation. Thr268 has been converted to alanine and the enzymatic properties and heme domain crystal structure determined. Using sodium laurate as the substrate, the mutant exhibited slower rates of O_2 and NADPH consumption. In addition, electron transfer is uncoupled from substrate hydroxylation as evidenced by the greater production of water and peroxide in the mutant compared to the wild-type enzyme. The crystal structure of the mutant reveals that the only changes in structure are confined to the site of mutation. These data indicate an important role for Thr268 in O_2 binding and activation in the metabolism of sodium laurate by cytochrome $P450_{BM-3}$.

Cytochrome P450 is a family of heme-containing monooxygenases involved in a variety of oxidative metabolic reactions. The P450 superfamily has been conceptually grouped into two subfamilies according to the electron transport system. Type I P450 monooxygenases require a three-protein system to utilize oxygen: the P450 heme protein, an iron−sulfur protein, and an FAD-containing reductase. Most of the bacterial P450s and mitochrondrial P450s belong to this family. Microsomal P450s are classified as type II P450s that are comprised of a heme protein and a NADPH−cytochrome P450 reductase containing both FAD and FMN.

The first example of a bacterial P450 that can be classifed as a type II P450 is $P450_{BM-3}$[1] isolated from *Bacillus megaterium*. In $P450_{BM-3}$, the heme and FAD/FMN reductase are fused as a catalytically self-sufficient fatty acid monooxygenase. $P450_{BM-3}$ catalyzes ω-n (n = 1−3) hydroxylation and epoxidation of long-chain fatty acids in the presence of O_2 and NADPH (Narhi & Fulco, 1986; Reuttinger & Fulco, 1981). The turnover number for fatty acid hydroxylation of $P450_{BM-3}$, 4600 min^{-1} in the case of pentadecanoic acid used as a substrate, is the highest of any P450 so far studied, probably because the covalent attachment of the heme and reductase domains results in faster intramolecular electron transfer. The two domains can be separated by limited tryptic digestion (Narhi & Fulco, 1986, 1987) or independently expressed in *Escherichia coli* (Boddupalli et al., 1992; Li et al., 1991). Recently it has been reported that nitric oxide synthase (NOS) has 71% amino sequence homology with the $P450_{BM-3}$ reductase domain and similar structural organization (Bredt et al., 1991; Lyons et al., 1992; White & Marletta, 1992). The heme domain of $P450_{BM-3}$ shows 17% sequence homology with $P450_{cam}$ and 41% sequence homology with microsomal $P450_{pcn}$ (Ruettinger et al., 1989). In view of higher sequence homology to microsomal P450 and the presence of a reductase domain containing FMN and FAD, $P450_{BM-3}$ has been classified as a type II P450. The crystal structure of the $P450_{BM-3}$ heme domain showed similar overall structural features with other bacterial P450s, $P450_{cam}$ and $P450_{terp}$, but with large differences observed in the substrate binding region (Hasemann et al., 1994; Li & Poulos, 1995; Ravichandran et al., 1993).

Although our understanding of the oxygen activation mechanism by the cytochromes P450 has rapidly advanced over the last few years, it still remains incomplete. Substrate binding often converts the enzyme from a low- to a high-spin form followed by reduction and oxygen binding. A second electron transfer step followed by O−O bond cleavage is thought to result in the formation of a high-valent iron−oxo complex which transfers the active oxygen to substrate through oxygen rebond with the other oxygen atom departing as hydroxide or water. Release of hydroxylated

[†] Supported in part by NIH Grants GM33775 (S.G.S.), GM31756 (S.G.S.), GM33688 (T.L.P.), and GM23913 (A.J.F.).

* Authors to whom correspondence should be addressed.

[⊗] Abstract published in *Advance ACS Abstracts,* October 15, 1995.

[1] Abbreviations: $P450_{BM-3}$, cytochrome P450 isolated from *Bacillus megaterium* (P450 CYP102); $P450_{cam}$, cytochrome P450 isolated from *Pseudomonas putida* (P450 CYP101); $P450_d$, rat liver microsomal cytochrome P450 (P450 1A2); $P450_{terp}$, cytochrome P450 isolated from *Pseudomonas sp.* (P450 108); $P450_{eryF}$, cytochrome P450 isolated from *Saccaropolyspora erthrea* (P450 107); FMN, flavin mononucleotide; FAD, flavin adenine dinucleotide; IPTG, isopropyl β-D-thiogalactopyranoside; GC−EIMS, gas chromatography−electron impact mass spectrometry.

0006-2960/95/0434-14733$09.00/0

substrate completes the catalytic cycle. Recently, a particular focus has been the nature of the acid catalytic group or groups which donate a proton to the departing oxygen atom following O−O bond scission. Unlike peroxidases, which contain an active site histidine for this purpose, P450s have none of the residues normally associated with acid−base catalysis suitably positioned for direct proton donation to the leaving oxygen atom. Much attention has focused on the P450 "distal helix" which is similarly positioned in P450s on the top of the heme plane and helps to form part of the oxygen binding site. Studies on the role of a conserved threonine residue in this I-helix have been carried out using site-directed mutagenesis on $P450_{cam}$ and several microsomal cytochrome P450s. THe crystal structure of $P450_{cam}$ showed that the side chain OH of the distal Thr forms a hydrogen bond with the carbonyl group of Gly248. Thus, if we consider this Thr as residue *n*, the side chain OH hydrogen bonds with the carbonyl oxygen atom of residue $n - 4$. This same pattern is maintained in $P450_{BM-3}$. Replacement of the threonine with alanine in $P450_{cam}$ abolished the hydroxylase activity and resulted in nearly complete uncoupling of NADH-derived reducing equivalents to the release of hydrogen peroxide (Imai et al., 1989; Martinis et al., 1989). Based on kinetic and crystallographic studies of the mutant enzyme (Imai et al., 1989; Martinis et al., 1989; Raag et al., 1991), Thr252 is thought to be involved in stabilization of the oxy complex and possibly plays a part in a proton shuttle mechanism. Similar mutagenesis experiments using microsomal enzymes yielded various results depending on the individual P450 species (Ishigooka et al., 1992). For instance, the Thr319 to Ala mutation in $P450_d$ results in an increased turnover number and a decrease in hydrogen peroxide formation comapred to wild-type protein when 7-ethoxycoumarin or acetanilide is a substrate yet the benzphetamine hydroxylation activity is diminished. A change in the overall substrate recognition events upon mutagenesis was observed in rabbit liver $P450_{3a}$ (Fukuda et al., 1993).

Here we report the construction, crystal structure, and catalytic properties of the $P450_{BM-3}$ mutant T268A, which corresponds to the T252A mutant of $P450_{cam}$. The crystal structure of the mutant heme domain reveals no significant change in active site toplogy in the substrate-free form. The Thr to Ala mutant of $P450_{BM-3}$ is found to result in a decrease in catalytic activity for fatty acid hydroxylation and an increase in the formation of hydrogen peroxide when laurate is used as substrate, analogous to that observed in $P450_{cam}$. The role of Thr268 in oxygen activation by $P450_{BM-3}$ is discussed.

EXPERIMENTAL PROCEDURES

Mutagenesis. Mutation of threonine 268 to alanine (T268A) was carried out by oligonucleotide-directed mutagenesis using the "Muta-gene phagemid *in vitro* mutagenesis kit" from Bio-Rad. For the mutagenesis reaction, we used pT7Bm3HdZ which has a gene encoding the heme domain of $P450_{BM-3}$ under the T7 RNA polymerase promoter (Darwish et al., 1991). Single-stranded DNA was generated in strain CJ236 transformed with pT7Bm3HdZ. A 21mer oligonucleotide with a threonine 268 to alanine mutation and an extra *Spe*I site, ACACGAAGCAACTAGTGGTCT, was synthesized at the genetic engineering facility at the University of Illinois and used without further purification. Mutation was confirmed with creation of a *Spe*I site and DNA sequencing reaction using the Sequenase 2.0 DNA sequencing kit from USB. A 0.74 kb *Afl*II−*Msc*I fragment containing the mutation point was subcloned into pUC13bm3 (Wen & Fulco, 1987) in order to construct pUC13bm3T268A which contains the gene encoding the intact protein and the upstream translation promoter region. *E. coli* strain DH5α and the Geneclean kit from Bio 101 were used for the subcloning of the 0.74 kb fragment into pUC13bm3.

Purification. The expression of wild-type and mutant heme domain proteins was carried out in *E. coli* strain JM109(DE3). Cells were grown in 2 × YT at 37 °C and induced with 0.4 mM IPTG at $OD_{600} = 1.0$. Cells were harvested 18 h after induction and kept at −70 °C for further use. Frozen cells were resuspended in lysis buffer (50 mM KP_i, pH 7.4, 0.1 mM EDTA, and 2 mM dithiothreitol containing lysozyme) and lysed at 4 °C overnight. Lysate was centrifuged at 37000*g* for 30 min to remove cell debris. Protein extract was diluted and loaded onto a DE52 column equilibrated with 30 mM potassium phosphate, pH 7.4, containing 2 mM DTT. $P450_{BM-3}$ heme domain protein was eluted with a 0−0.4 M KCl gradient in 30 mM potassium phosphate buffer at pH 7.4 containing 2 mM DTT. Fractions containing heme protein were collected and concentrated with YM10 membranes (Amicon, MWCO = 10 000). Concentrated protein was loaded onto a S-200 gel filtration column, eluted with 0.1 M KP_i, pH 7.4, and further purified by FPLC using a DEAE column with a 0−0.4 M KCl gradient. Fractions with $R_z(A_{418}/A_{280}) > 1.5$ were pooled and used. Intact proteins of wild-type and T268A mutants of $P450_{BM-3}$ were expressed in DH5α in LB and purified by the same method except a potassium phosphate gradient (30−400 mM) was used for the anion exchange column to prevent the loss of flavin during the purification (Klein & Fulco, 1993). For intact protein, fractions with $R_z(A_{418}/A_{280}) > 0.6$ were collected. SDS−PAGE was performed using the Pharmacia phast gel system to confirm the protein size and purity.

Analytical Procedures. Protein concentration was determined with the dithionite-reduced CO difference spectrum ($\epsilon_{450} = 91\,000\ M^{-1}\ cm^{-1}$) and the alkaline pyridine−hemochromogen assay using 20% v/v pyridine and 0.1 N NaOH (Omura & Sato, 1964). In computing the heme concentration, a value of 32 400 $M^{-1}\ cm^{-1}$ was used for the difference in molar extinction between 557 and 575 nm in the dithionite reduced-minus-oxidized difference spectrum of the hemochromogen. Total protein concentration was determined by the biuret method. The amount of FAD in the intact protein was determined using the ferricyanide reductase assay. Ferricyanide reductase activity was measured in 0.1 M KP_i, pH 7.4, 500 nmol of $K_2Fe(CN)_6$, and 150 μM NADPH using $\epsilon_{420} = 1020\ M^{-1}\ cm^{-1}$.

Electronic absorption spectra were obtained with a Hitachi U-3300 spectrometer using a scan rate of 600 nm/min; 10 mM sodium laurate stock solution was prepared in 50 mM Na_2CO_3. The spectra of substrate-bound forms were obtained in 0.5 M KP_i, pH 8.0, in the presence of sodium laurate with a final concentration of 200 μM.

Enzyme Assays. The rate of NADPH oxidation was measured by monitoring the absorbance change at 340 nm using an extinction coefficient of 6220 $M^{-1}\ cm^{-1}$. The reaction was initiated with the addition of 150 μM NADPH to the reaction mixture, 0.1 M KP_i, pH 8.0, with 200 μM

sodium laurate, and varying amounts of protein. The NADPH oxidation rate was calculated with the data obtained for the first 30 s of the reaction.

Oxygen consumption rates were measured with 150 μM NADPH and 200 μM sodium laurate in 0.1 M KP_i, pH 8.0, using a Clark-type oxygen electrode (YSI membrane). Buffer solution was saturated with air before use, and the residual electrode response was measured in the presence of dithionite (concentration of oxygen in air-saturated aqueous solution = 237 μM).

To measure the production rate of hydrogen peroxide, the oxygen consumption rate was measured in the presence of 25 μg of catalase in the reaction mixture. The stoichiometric amount of hydrogen peroxide produced was measured with a horseradish peroxidase based assay. The reaction mixture (0.5 μM enzyme, 150 μM NADPH, and 200 μM sodium laurate in 0.1 M KP_i, pH 7.4) was withdrawn with a gas-tight syringe immediately after the addition of NADPH. One milliliter samples were squirted into a tube containing 0.1 mL of 1 N HCl to stop the reaction at 0.5 min intervals. The reaction mixture was neutralized with 100 μL of 1 N NaOH. Addition of 10 mM 2,2′-azinobis(3-ethylbenzothiazoline-6-sulfonic acid) (ABTS) was followed with addition of 5 μL of 5 mg/mL horseradish peroxidase. The amount of oxidized ABTS was measured using the absorbance at 406 nm.

The amount of extra water produced by uncoupling (Atkins & Sligar, 1987) was measured using a special cell which allowed simultaneous measurement of oxygen and NADPH concentration. A Clark-type electrode was interfaced through a BAS 27 electrometer to a data logging system composed of HP voltmeters and a personal computer running Lab Windows.

For product analysis, the reaction (0.5 μM enzyme, 150 μM NADPH, and 100−200 μM sodium laurate in 0.1 M KP_i, pH 7.4; total volume of 2 mL) was stopped with addition of 200 μL of 1 N HCl after incubation for 5 min at room temperature. The 2 mL reaction mixture was twice-extracted with 5 mL of diethyl ether. Solvent was removed with a stream of nitrogen, and the substrate and product were methylated with etheral diazomethane solution at room temperature. Diazomethane was produced with a microscale diazomethane generator using MNNG (1-methyl-3-nitro-1-nitrosoguanidine) as a precursor. Excess diazomethane and solvent were removed under nitrogen. The derivatized product and substrate were dissolved in 30 μL of CH_2Cl_2 and analyzed with GC (DB-23, J&W program: 70 °C, 2 min; 70−220 °C, 5 °C/min) using 12-hydroxylaurate and methyl laurate as standards and confirmed with GC−EIMS (DB5).

Crystallography. The T268A mutant of the $P450_{BM-3}$ heme domain protein was crystallized under the identical condition used for the wild-type heme domain (Li & Poulos, 1995; Ravichandran et al., 1993). Sitting drops were set up by adding equal volumes of protein at 40 mg/mL and the reservoir solution of 16% PEG8000 and 100 mM $MgSO_4$ in 100 mM PIPES, pH 6.8. Preequilibrated drops were streak-seeded with the wild-type heme domain crystals. X-ray diffraction data were collected on a Siemens X-1000 area detector with a rotating-anode CuKα X-ray generator and a double-mirror focusing optic. The raw data were proceeded with XENGEN (Howard et al., 1987). The initial $F_o - F_c$ difference Fourier was dominated by negative difference density around the Thr268 side chain, so this residue was replaced by Ala for further refinement. XPLOR (Brunger, 1992) was used for conventional positional and temperature factor refinement and TOM for graphics modeling (Cambilliu & Horjales, 1987). Noncrystallographic symmetry restraints were not imposed during the refinement, enabling two separate views of the mutation site in the two molecules in the asymmetric unit. Statistics of data collection and refinement of the mutant heme domain structure are shown in Table 1.

Table 1: Statistics of Data Collection and Refinement of the T268A Mutant of $P450_{BM-3}$ Heme Domain Protein

cell parameters	a = 59.5 Å, b, 154.0 Å, c = 62.4 Å, β = 95.0°
space group	$P2_1$
no. of observations	120931
no. of independent reflections	44522
R_{merge} (%)	8.00
data completeness (%) at	
50.0−3.6 Å	99.6
3.6−2.9 Å	95.6
2.9−2.7 Å	89.3
2.7−2.4 Å	81.6
2.4−2.3 Å	62.5
no. of reflections used in refinement with $F > 2\sigma(F)$	37057
resolution range of refinement (Å)	10.0−2.3
$R = \sum\|\|F_o\| - \|F_c\|\|/\sum\|F_o\|$ (%)	17.2
no. of protein atoms	7424
no. of water molecules	397
rms in bond lengths (Å)	0.008
rms in bond angles (deg)	1.41
coordinate error (Luzzati plot) (Å)	0.25

RESULTS

Enzyme Characterization. The intact protein of T268A mutant was purified using the same procedure employed for the wild-type protein. During the purification, some partial degradation of the protein was observed, but the degraded protein was readily removed using a final FPLC step. Analysis by SDS/PAGE revealed that the purified enzyme was free of small polypeptide contamination after FPLC. To avoid the loss of FMN, a phosphate gradient instead of a KCl gradient was used to purify the intact protein (Klein & Fulco, 1993). Determination of heme content in the purified protein utilized a dithionite-reduced CO difference spectrum and pyridine−hemochromogen assay. The CO complex formed after dithionite reduction showed the characteristic 450 nm peak in both the wild-type and mutant proteins (ϵ_{450} = 91 000 M^{-1} cm^{-1}). The heme content from the reduced CO difference spectrum agreed well with that of the pyridine−hemochromogen assay. Ferricyanide reductase activities of wild-type and mutant are comparable to reported values (Klein & Fulco, 1993), implying the full incorporation of FAD in wild-type and mutant proteins.

The electronic absorption spectra of the purified protein are shown in Figure 1. The intact $P450_{BM-3}$ (T268A) mutant has a characteristic shoulder between 450 and 550 nm, indicating the presence of flavin with a Soret band at 418 nm in the absence of substrate. The addition of substrate to the purified protein caused a shift of λ_{max} to 389 nm, indicating low- to high-spin conversion. The electronic absorption spectra of the Thr268Ala mutant were indistinguishable from wild-type enzyme in the oxidized form with and without substrate, the reduced form, and the reduced CO complex.

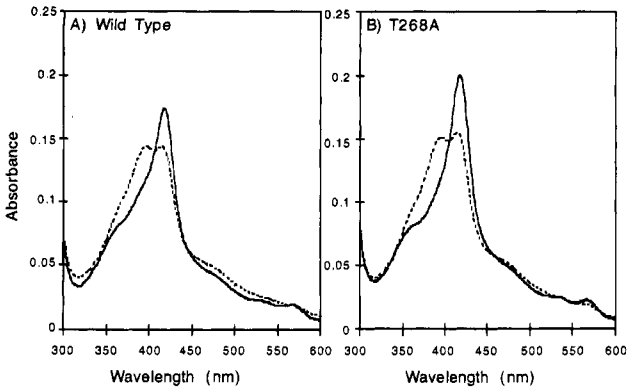

FIGURE 1: UV−Vis absorption spectra of oxidized and substrate (laurate)-bound forms of $P450_{BM-3}$: (A) wild type; (B) T268A mutant. Spectra were taken in 0.5 M KP_i, pH 8.0. Solid line, oxidized form. Dashed line, laurate-bound form.

Table 2: Kinetic and Stoichiometric Parameters for $P450_{BM-3}$ Reaction[a]

	wild type	T268A
NADPH oxidation rate[b]	948	268
O_2 consumption rate[b]	951	236
hydroxylaurate[c]	106 ± 7	16 ± 1
H_2O[c]	ND[d]	11
H_2O_2[c]	ND	67

[a] Details of the reaction conditions are explained under Experimental Procedures. [b] NADPH oxidation rate and O_2 consumption rate are shown as nanomoles of metabolite produced per minute per nanomoles of enzyme used. [c] Stoichiometry of the product is calculated as a percentage of product measured to NADPH utilized. The amount of hydroxylated laurate is the sum of three isomers: ω-1, ω-2, and ω-3 hydroxylaurate. [d] ND, not detected.

Enzyme Activity. For the kinetic studies of wild-type and mutant enzymes, sodium laurate was chosen as the substrate since this is the most soluble fatty acid substrate and also since laurate is known not to yield further oxidation products after the initial monooxygenation. In the case of fatty acids longer than myristic acid, subsequent oxidation of the initial product has been reported (Boddupalli et al., 1990).

Table 2 presents the rate of NADPH oxidation when NADPH is limiting in the laurate monooxygenase assay mix. Also shown in Table 2 and in Figure 2 is the rate of O_2 consumption measured using an oxygen electrode. In a perfectly coupled system, these rates should be equal, giving one NADPH oxidized per O_2 consumed. Since four electrons are required to reduce O_2 to water, a ratio greater than 1 indicates that there is uncoupling to an oxidase pathway where the O_2 is reduced to water. The ratio of NADPH to O_2 is 0.96 for wild type, indicating no water formation. In T268A, the ratio of NADPH to O_2 is 1.11, indicating that a small fraction of NADPH reducing equivalents are used to reduce O_2 to water.

Uncoupling may still be present even if the rates of NADPH oxidation and O_2 consumption are equal and if the NADPH reducing equivalents are directed toward peroxide formation. The level of uncoupling of O_2 to hydrogen peroxide was determined in two ways. First, the change in the concentration of oxygen was measured in the presence and the absence of catalase (Figure 2, Table 2), and second, a direct measure of H_2O_2 formed was performed using a horseradish peroxidase-based assay (Table 2). In the wild-type enzyme, there was no increase in oxygen concentration

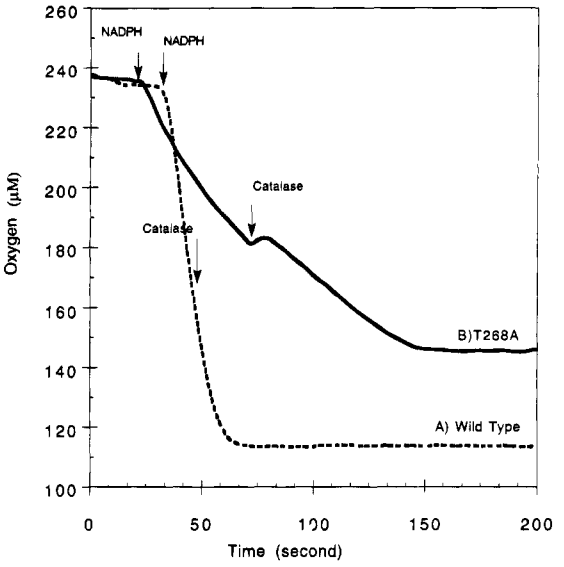

FIGURE 2: O_2 consumption rate of $P450_{BM-3}$ (A) wild type and (B) T268A mutant in the presence of 200 μM laurate at pH 8.0, in 0.1 M KP_i. Addition of 150 μM NADPH and catalse is indicated by arrows.

when catalase was added 20 s after the initiation of the reaction with NADPH. Increasing the protein concentration does not lead to the formation of hydrogen peroxide. While wild-type enzyme showed no hydrogen peroxide formation, the addition of catalase to the reaction mixture of the T268A mutant gave an immediate increase in oxygen concentration due to the disproportionation of hydrogen peroxide to O_2 and H_2O. Addition of catalase in the mutant reaction mixture prior to NADPH addition showed a decrease in the O_2 consumption rate, an observation that can be explained by the *in situ* conversion of hydrogen peroxide to O_2 by catalase (data not shown). As shown in Table 2, in the T268A mutant, 67% of the reducing equivalents go toward H_2O_2 formation.

Analysis of Products. As shown in Table 2, the T268A mutant gives about 16% yield of product after 5 min of reaction relative to the amount of NADPH utilized while all of the laurate is converted to product for the wild-type enzyme. However, the distribution of products is the same in both wild-type and mutant enzymes (data not shown). This correlates well with the uncoupling data described in the previous section and indicates that a significant fraction of NADPH reducing equivalents are not utilized for substrate hydroxylation in the T268A mutant. The wild-type enzyme does not appear to have significant inherent catalase activity under conditions of these experiments.

Mutant Crystal Structure. The isolated heme domains of the wild type and T268A mutant were produced as described by Li et al. (1991). The various spectroscopic properties used to characterize the holoenzymes also were employed for analysis of the mutant heme domain. As with the holoenzyme, the various spectral properties of the wild-type and mutant heme domains were the same. Moreover, the crystallization behavior of the mutant heme domain protein was identical to wild type, exhibiting the same crystal morphology and isomorphous cell parameters (Table 1). There are two molecules in the asymmetric unit, thereby providing two independent views of changes that are caused by the mutation.

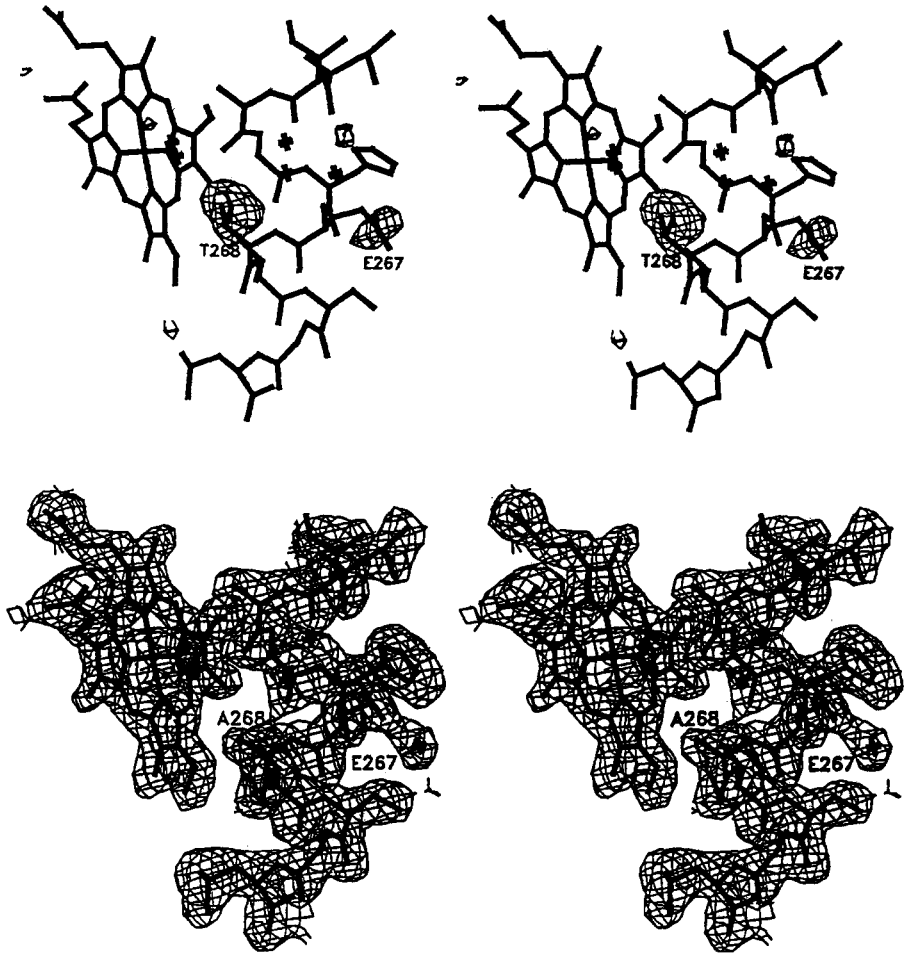

FIGURE 3: (A, top) Stereoview of the initial $F_o - F_c$ negative difference electron density (contoured at 3σ, molecule B shown only) constructed with the T268A mutant diffraction data against the refined model of the wild-type $P450_{BM-3}$ heme domain. The negative density around the Thr268 side chain indicates the new identity of the alanine residue that has been engineered into place. (B, bottom) The final $2F_o - F_c$ electron density (contoured at 1σ) overlaid with the refined model of the T268A mutant heme domain protein. Note that there is no new water molecule next to Ala268. Also, the side chain conformation of Glu267 has been changed and switched with an H-bonded water molecule (residue 859) compared to that in the wild-type structure. No similar conformational change was observed for the Glu267 side chain in molecule A.

The initial $F_o - F_c$ difference electron density map (Figure 3) was calculated using the mutant intensity data, and calculated structure factors were from the refined wild-type heme domain (Li & Poulos, 1995). The bulky negative differences densities surrounding the side chains of Thr268 in both molecules were clearly observed, confirming the identity of the mutated alanine residue. The only other difference density was around Glu267 in molecule B, indicating multiple conformations of this side chain. However, a neighboring water molecule makes precise determination of the multiple positions of the Glu side chain difficult. Water 859 hydrogen bonds with the carboxylate of Glu267, and it appears that in one conformer the carboxylate group swings over to occupy the position of water 859.

The overall root mean square deviations of the main chain atoms between the wild type and T268A mutant $P450_{BM-3}$ heme domain are less than 0.18 Å. The structural changes on protein molecules around the mutation sites are minimal except for the conformational change of the Glu267 side chain in molecule B. Although the hydrogen bond between the Thr268 hydroxyl oxygen atom and the Ala264 carbonyl oxygen atom is no longer present in the T268A mutant structure, the Ala264 carbonyl group still makes a strong hydrogen bond to the axial water or hydroxyl ligand coordinated to the iron. Unlike in the crystal structure of the T252A mutant of $P450_{cam}$ (Raag et al., 1991), no extra ordered water molecule was found in place of the missing Thr268 side chain OH group. Although the ordered water molecule (residue 709 in molecule A and 622 in B) in the widened helical grove shifted slightly toward the missing threonine side chain, the cavity left by the missing threonine side chain still remained empty (Figure 3). This, of course, does not preclude the possibility that highly mobile waters not visible crystallographically now occupy the additional space left by the missing OH group.

DISCUSSION

Uncoupling in P450s. The reaction cycle of hydroxylation by cytochrome P450 is shown in Figure 4. The first two electron transfer steps reduce molecular oxygen to a hypothetical peroxo complex. Protonation and O–O bond cleavage generate the active oxygen species that is responsible for the monooxygenation reaction. Three uncoupling pathways are shown in the reaction cycle: superoxide, hydrogen peroxide, and water formation. In $P450_{cam}$, the iron-bound oxygen is used solely to hydroxylate camphor.

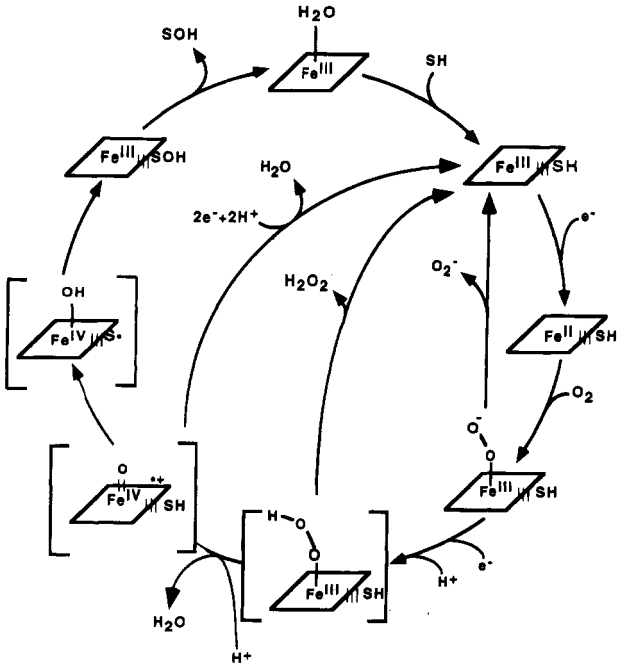

FIGURE 4: P450 reaction cycle. SH: substrate. SOH: hydroxylated product.

In contrast, uncoupling of oxygen to hydrogen peroxide is a commonly observed process in microsomal P450s. Formation of hydrogen peroxide can be rationalized by release from a putative iron−peroxo complex prior to the formation of the high-valent iron−oxo species through O−O bond scission. Another known uncoupling pathway is an oxidase pathway which forms water by the four-electron reduction of dioxygen.

Of central importance in understanding the O−O bond cleavage reaction and uncoupling is the nature of the acid catalyst that donates a proton to the hypothetical peroxo intermediate. A majority of research has focused on the I-helix residues and, in particular, the highly conserved Thr residue which participates in a hydrogen bonding pattern near the O_2 site that is part of a local helical distortion. This distortion appears in the three P450 structures that have a Thr at this position (Hasemann et al., 1994; Poulos et al., 1987; Ravichandran et al., 1993) and also in the one example where the Thr is replaced by Ala (Cupp-Vickery & Poulos, 1995).

Thr Mutants in P450$_{cam}$. The role of the distal Thr residue has been the subject of several studies in various P450s. Not unexpectedly, most of the data derive from studies with P450$_{cam}$. In the crystal structure of the ternary camphor−CO−P450$_{cam}$ complex, the threonine contacts both substrate and ligand. Kinetic and structural properties of the T252A mutant of P450$_{cam}$ revealed that the presence of the threonine is necessary for the efficient hydroxylation of camphor (Imai et al., 1989; Martinis et al., 1989). The NADH oxidation rate and O_2 consumption rate of the mutant are similar to those of wild type, but the rate of autoxidation is an order of magnitude faster than wild type. One of the proposed roles of the threonine is stabilization of the oxygen-bound intermediate through the formation of a hydrogen bond to the iron-bound oxygen. The loss of the hydroxyl group reduces the stability of the oxygen-bound intermediate, resulting in the release of superoxide and loss of catalytic activity. The other major effect of the mutation is that very little product is formed. Over 95% of the oxygen is recovered as hydrogen peroxide. The crystal structure of the mutant showed rearrangement of solvent structure near the active site with one extra water molecule and a further widening of the local helical distortion in helix I (Raag et al., 1991). It was suggested that the extra solvent molecule is responsible for the uncoupling of enzyme turnover by supplying proton in an uncontrolled manner.

Recently, Kimata et al. reported the incorporation of an unnatural amino acid in place of Thr252 in P450$_{cam}$ using an *in vitro* protein synthesis system (Kimata et al., 1995). Here Thr252 was replaced with methoxythreonine where the side chain OH has a methyl group added. This mutant showed one 5-*exo*-hydroxylcamphor product formed per O_2 consumed, indicating a fully coupled system. This is the first mutant where a larger side chain than Thr has been introduced at position 252 and should preclude additional solvent from moving into the active site as was found in the T252A mutant and might account for the lack of uncoupling. However, this study raises serious doubts on the role of Thr252 as the direct proton donor to the iron-linked oxygen. Kimata et al. (1995) conclude that the hydroxyl group of threonine 252 is not a prerequisite for O−O bond scission and proposed a hypothetical proton relay system in which the side chain oxygen of threonine is hydrogen-bonded to water instead of the hydroxyl group of threonine 252. Such a model is consistent with the proton inventory and kinetic solvent isotope results of Akins and Sligar (1994).

Thr Mutants in Eukaryotic P450s. Further insights into the role of the conserved Thr derive from site-directed mutagenesis studies with eukaryotic P450s. Thr319 in P450$_d$ is expected to occupy the same position as Thr252 in P450$_{cam}$ (Furuya et al., 1989). The catalytic activities of the T319A mutant in P450$_d$ toward 7-ethoxycoumarin, acetanilide, and 17β-estradiol are higher than the wild type whereas there is no catalytic activity toward benzphetamine (Furuya et al., 1989; Ishigooka et al., 1992). T319A mutant autoxidized at the same rate as wild type, and a decrease in hydrogen peroxide formation and a higher coupling to hydroxylated product also were observed. The role of threonine in microsomal P450$_d$ was suggested to be in the recognition of the substrate rather than the stabilization of the oxygen-bound complex. This is further supported from the studies using the asymmetrical axial ligand (Krainev et al., 1993) since Thr319 appears to be important for discriminating between chiral axial ligands.

Role of Threonine 268 in P450$_{BM-3}$. Results from the present study show that the Thr-to-Ala mutant in P450$_{BM-3}$ affects catalytic activity between the two extremes of P450$_{cam}$ and P450$_d$. Unlike P450$_{cam}$, where the hydroxylated product is not observed, the T268A mutant of P450$_{BM-3}$ gave 16% product formation relative to the amount of NADPH used. Therefore, like P450$_d$, P450$_{BM-3}$ is less sensitive to the Thr-to-Ala substitution. One very obvious difference between P450$_{cam}$ and P450$_{BM-3}$ is that P450$_{BM-3}$ has an extra Thr immediately following the distal Thr268 (P450$_{BM-3}$ numbering). The presence of a threonine cluster in the conserved I-helix is a common feature of eukaryotic P450s. In the P450$_{BM-3}$ heme domain crystal, both Thr268 and Thr269 participate in side chain−backbone hydrogen bonds (Li & Poulos, 1995; Ravichandran et al., 1993). Besides the threonine to carbonyl hydrogen bonding, water molecules

in the helical groove are involved in stabilizing the local helical distortion. Whether the hydroxyl group of threonine 269 can stabilize the intermediate in the absence of threonine 268 is not known. Another feature in common is the relatively broad substrate specificity of $P450_d$ and $P450_{BM-3}$ compared to $P450_{cam}$. $P450_{BM-3}$ is capable of monooxygenation of saturated and unsaturated long-chain fatty acids, alcohols, and amides with different product distribution depending on the length of the carbon chain and the position of the double bond (Miura & Fulco, 1975; Narhi & Fulco, 1986). This broad substrate specificity implies that the active site of $P450_{BM-3}$ is quite flexible. Although the active site of $P450_{BM-3}$ reflects high flexibility, it should be noted that there is no uncoupling pathway to either hydrogen peroxide or water formation in the wild-type protein. When palmitate is used as substrate for the T268A mutant of $P450_{BM-3}$, we observe less decrease in the rate of NADPH oxidation and O_2 consumption. However, formation of hydrogen peroxide also is observed in the palmitate reaction. The presence of threonine is necessary in complete coupling of the hydroxylation reaction by $P450_{BM-3}$ with both laurate (12 carbons) and palmitate (16 carbons). The degree of uncoupling in the mutant appears to vary with the substrate, as expected from the change in product distribution which depends on the length of the fatty acid carbon chain.

Recent NMR studies on the $P450_{BM-3}$ heme domain by Modi et al. (1995) show that the exchangeable proton lies closer to the heme iron in the laurate-bound form of $P450_{BM-3}$ than in the substrate-bound form of $P450_{cam}$. Relaxation measurements on the substrate protons lead to a 7.6−7.8 Å distance between the iron and substrate. Since this is much too far for direct attack of an iron−oxo complex on the ω/ω-3 positions, it is may be that the substrate repositions in the active site during catalysis. Clearly, it is of interest to determine whether this is due to the presence of a reductase domain or electron transfer during the catalytic cycle.

Summary, Conclusions, and Speculations. The diversity of results obtained from the various distal Thr substitutions would at first preclude some universal role played by the distal Thr in all P450s. Indeed, Hasemann et al. (1995) carried out a detailed comparison of $P450_{BM-3}$, $P450_{terp}$, and $P450_{cam}$ and noted subtle but distinct differences in the distal helix, particularly around the distal Thr. $P450_{terp}$ and $P450_{BM-3}$ more closely resemble one another than they do $P450_{cam}$, and these differences were used to argue that the various roles proposed for the distal Thr based on $P450_{cam}$ may not be generally applicable to all P450s. For example, Hasemann et al. (1995) noted that a distal helix I peptide carbonyl oxygen−axial water ligand H-bond present in $P450_{BM-3}$ and $P450_{terp}$ occludes the O_2 binding site relative to $P450_{cam}$. However, when substrates bind to either $P450_{BM-3}$ or $P450_{terp}$, the axial water (or hydroxide) ligand is displaced by the substrate as evidenced by the shift to the high-spin state when substrates bind (Boddupalli et al., 1992; Narhi & Fulco, 1986). As a result, the backbone−axial water ligand H-bond observed in the substrate-free structures is unlikely to be present in the substrate-bound complexes. The catalytically relevant structures that must be compared are the substrate-bound complexes, and until these are available for $P450_{BM-3}$ and $P450_{terp}$, one cannot draw meaningful mechanistic conclusions regarding subtle differences in the I-helix hydrogen bonding pattern in comparing the known P450 structures. Obviously, the one common thread that links the mutagenesis results is that replacing the distal Thr with a residue that cannot form hydrogen bonds results in various degrees of uncoupling. The very recent and exciting result, where the distal Thr was replaced with methoxy-Thr (Kimata et al., 1995), yet is still very active giving the expected product, indicates that the distal Thr is very likely not the direct proton donor to the iron-linked oxygen, which is consistent with published solvent isotope effects which show a KSIE of 1.8 with two or more protons in flight in the transition state (Aikens & Sligar, 1994).

That water may in fact be the direct proton donor is further evidenced by the recent crystal structure determination of $P450_{eryF}$ with substrate bound (Cupp-Vickery & Poulos, 1995). This is the second P450 structure solved with substrate bound and the first where an Ala replaces the distal Thr. Even with this important change in sequence, the I-helix still has a local distortion. The substrate for $P450_{eryF}$, 6-deoxyerythronolide, is so large (27 non-hydrogen atoms) that the distal I-helix threonine cannot be tolerated owing to steric restraints. This could help to explain why, in other P450s, mutations of the distal Thr lead to changes in substrate specificity. More relevant to the present discussion, however, is the H-bonded network near the oxygen binding site. Even though $P450_{eryF}$ does not have a distal Thr, a water molecule takes the place of the Thr side chain OH. As a result, $P450_{eryF}$ has a H-bonded network very similar to that found in $P450_{cam}$. However, $P450_{eryF}$ has a new water not observed in $P450_{cam}$ that is situated only 3.8 Å from the iron atom. Any diatomic ligand would either displace or, more interestingly, directly interact with this water molecule. A detailed analysis of the H-bonding donor/acceptor arrangement in $P450_{eryF}$ shows that this water close to the iron has one hydrogen atom available to serve as an H-bond donor (Cupp-Vickery & Poulos, 1995). This could well be the acid catalyst required for O−O bond cleavage. Although the evidence for $P450_{cam}$ is not so direct, there are indications that potentially important groups are involved with protein−water interactions. Using osmotic pressure methodologies, it has been demonstrated that water is clearly involved in the key catalytic steps of the $P450_{cam}$ reaction cycle. One of the most interesting set of studies is mutations of the highly conserved acidic amino acid, Asp251 in $P450_{cam}$, that immediately precedes the distal Thr in most P450s. The Asp251Asn mutant in $P450_{cam}$ leads to a large drop in activity but not uncoupling (Gerber & Sligar, 1994). Moreover, Asp251 is known to be flexible, and in at least one $P450_{cam}$−inhibitor complex, Asp251 swings in toward the active site to form an H-bond with a new water molecule (Poulos et al., 1987). Therefore, while the effects of the various Thr mutations have been interpreted primarily in terms of protein structure, the analysis also should extend to local solvent structure. The change in local water structure and H-bonded network in response to various mutations should be expected to differ widely in various P450s owing to the various size, shape, and polar properties of different substrates. Thus, the distal Thr could be playing a similar role in all P450s, but its importance necessarily must vary depending on the stereochemical properties of the substrate. The elusive search for the catalytic group could end with something as seemingly simple and complex as water.

REFERENCES

Aikens, J., & Sligar, S. G. (1994) *J. Am. Chem. Soc. 116*, 1143−1144.

Atkins, W. M., & Sligar, S. G. (1987) *J. Am. Chem. Soc. 109*, 3754−3760.

Boddupalli, S. S., Estabrook, R. W., & Peterson, J. A. (1990) *J. Biol. Chem. 265*, 4233−4239.

Boddupalli, S. S., Pramanik, B. C., Slaughter, C. A., Estabrook, R. W., & Peterson, J. A. (1992) *Arch. Biochem. Biophys. 292*, 20−28.

Bredt, D. S., Hwang, P. M., Glatt, C. E., Lowenstein, C., Reed, R. R., & Snyder, S. H. (1991) *Nature 351*, 714−718.

Brunger, A. T. (1992) *X-PLOR Version 3.1. A system for X-ray crystallography and NMR*, Yale University Press, New Haven, CT.

Cambilliu, C., & Horjales, E. (1987) *J. Mol. Graphics 5*, 174−177.

Cupp-Vickery, J. R., & Poulos, T. L. (1995) *Nat. Struct. Biol. 2*, 144−153.

Darwish, K., Li, H., & Poulos, T. L. (1991) *Protein Eng. 4*, 701−708.

DiPrimo, C., Sligar, S. G., Hui Bon Hoa, G., & Douzou, P. (1992) *FEBS Lett. 312*, 252−254.

Fukuda, T., Imai, Y., Komori, M., Nakamura, M., Kusunose, E., Satouchi, K., & Kusunose, M. (1993) *J. Biochem. 113*, 7−12.

Furuya, H., Shimizu, T., Hirano, K., Hatano, M., Fujii-Kuriyama, Y., Raag, R., & Poulos, T. L. (1989) *Biochemistry 28*, 6848−6857.

Gerber, N. C., & Sligar, S. G. (1994) *J. Biol. Chem. 269*, 4260−4266.

Hasemann, C. A., Ravichandran, K. G., Peterson, J. A., & Diesenhofer, J. (1994) *J. Mol. Biol. 236*, 1169−1185.

Hasemann, C., Kurumbail, R. G., Boddupalli, S. S., Peterson, J. A., & Deisenhofer, J. (1995) *Structure 3*, 41−62.

Howard, A. J., Gilliland, G. L., Finzel, B. C., Poulos, T. L., Ohlendorf, D. H., & Salemme, F. R. (1987) *J. Appl. Crystallogr. 20*, 383−387.

Imai, M., Shimada, H., Watanabe, Y., Matsushima-Hibiya, Y., Makino, R., Koga, H., Horiuchi, T., & Ishmura, Y. (1989) *Proc. Natl. Acad. Sci. U.S.A. 86*, 7823−7827.

Ishigooka, M., Shimizu, T., Hiroya, K., & Hanato, M. (1992) *Biochemistry 31*, 1528−1531.

Kimata, Y., Shimada, H., Hirose, T., & Ishimura, Y. (1995) *Biochem. Biophys. Res. Commun. 208*, 96−102.

Klein, M. L., & Fulco, A. J. (1993) *J. Biol. Chem. 268*, 7553−7561.

Krainev, A., Shimizu, T., Ishigooka, M., Hiroya, K., & Hanato, M. (1993) *Biochemistry 32*, 1951−1957.

Li, H., & Poulos, T. L. (1995) *Acta Crystallogr. D51*, 21−32.

Li, H., Darwish, K., & Poulos, T. L. (1991) *J. Biol. Chem. 266*, 11909−11914.

Lyons, C. R., Orloff, G. J., & Cunningham, J. M. (1992) *J. Biol. Chem. 267*, 6370−6374.

Martinis, S. A., Atkins, W. M., Stayton, P. S., & Sligar, S. G. (1989) *J. Am. Chem. Soc. 111*, 9252−9253.

Miura, Y., & Fulco, A. J. (1975) *Biochim. Biophys. Acta 388*, 305−317.

Modi, S., Primrose, W. U., Boyle, J. M. B., Gibson, C. F., Lian, L.-Y., & Roberts, G. C. K. (1995) *Biochemistry 34*, 8982−8988.

Narhi, L. O., & Fulco, A. J. (1986) *J. Biol. Chem. 261*, 7160−7169.

Narhi, L. O., & Fulco, A. J. (1987) *J. Biol. Chem. 262*, 6683−6690.

Omura, T., & Sato, R. (1964) *J. Biol. Chem. 239*, 2370−2378.

Poulos, T. L., Finzel, B. C., & Howard, A. J. (1987) *J. Mol. Biol. 195*, 687−700.

Raag, R., Martinis, S. A., Sligar, S. G., & Poulos, T. L. (1991) *Biochemistry 30*, 11420−11429.

Ravichandran, K. G., Bouddupalli, S. S., Hasemann, C. A., Peterson, J. A., & Deisenhofer, J. (1993) *Science 261*, 731−736.

Reuttinger, R. T., & Fulco, A. J. (1981) *J. Biol. Chem. 256*, 5728−5734.

Ruettinger, R. T., Wen, L.-P., & Fulco, A. J. (1989) *J. Biol. Chem. 264*, 10987−10995.

Wen, L.-F., & Fulco, A. J. (1987) *J. Biol. Chem. 262*, 6676−6682.

White, K. A., & Marletta, M. A. (1992) *Biochemistry 31*, 6627−6631.

BI951299E